IJC Heart & Vasculature 31 (2020) 100672

Contents lists available at ScienceDirect

IJC Heart & Vasculature

journal homepage: www.journals.elsevier.com/ijc-heart-and-vasculature

Correspondence

Characterisation of an atherosclerotic micro-calcification model using ApoE$^{-/-}$ mice and PET/CT

1. Introduction

Intraplaque calcification is a prominent feature of advanced atherosclerotic plaque development. Current clinical evidence suggests that the size of calcium deposit may confer different effects on plaque stability [1–3]. Macro-calcified deposits (CT detected) are thought to confer plaque stability whereas micro-calcification ([^{18}F]NaF PET detected) are thought to be a feature of high-risk 'vulnerable' plaques which are prone to rupture. Following on from the emerging role of micro-calcification in high risk plaques within the clinic [4], there is now an urgent need for preclinical atherosclerotic models with this feature to gain mechanistic insights and assess the impact of calcification-targeted therapies. Using a combination of invasive and *ex vivo* methods, ApoE$^{-/-}$ mice placed on an atherogenic diet have been shown to develop intraplaque calcification [5]. Additionally, [^{18}F]NaF PET/CT has been used to assess the impact of exercise on calcification in ApoE$^{-/-}$ mice on a western diet [6]. In this study, we set out to determine if [^{18}F]NaF PET/CT could be used to non-invasively detect and quantify micro-calficiation in the ApoE$^{-/-}$ high cholesterol diet (HCD) mouse model, and examine the temporal nature of this process.

2. Methods

All experiments were authorized by the local University of Edinburgh animal welfare and ethical review committee and in accordance with the Home Office Animals (Scientific Procedures) Act 1986. Male ApoE$^{-/-}$ mice at 10–12 weeks of age were placed on a HCD (D12336, Research Diets Inc., USA) for up to 12 weeks. The animals were housed under standard 12 h light:12 h dark conditions with food and water available *ad libitum*. *In vivo* PET/CT was performed at 6 and 12 weeks post-commencement of HCD. Anaesthesia was induced and maintained using 1.5–2.5% isoflurane (50/50 oxygen/nitrous oxide, 1 l/min). Body temperature was maintained by heated scanner bed or heated mat and monitored by rectal thermometer. [^{18}F]NaF (2.3–7.5 MBq) was administered via intraperitoneal injection (0.2–0.3 ml). Immediately following radiotracer administration, a 60 min scan was performed on a nanoPET/CT (Mediso, Hungary) using 3-dimentional 1:5 mode. A CT scan (semi-circular full trajectory, maximum field of view, 480 projections, 50 kVp, 300 ms and 1:4 binning) was acquired for attenuation correction. Scans were reconstructed using Mediso's iterative Tera-Tomo 3D reconstruction algorithm, which includes point spread correction, and the following settings: 4 iterations, 6 subsets, full detector model, low regularization, spike filter on, voxel size 0.4 mm and 400–600 keV energy window. At the end of the PET/CT scan mice were culled and their aorta harvested for *ex vivo* analysis.

Post-mortem aortas were excised from the aortic root, along the arch (while keeping the initial portion of branches attached) and down through the descending aorta to the abdominal aorta. Sections of the brachiocephalic trunk were wax processed, sectioned and stained using Masson's trichrome before the stenosis ratio was calculated by measuring the area of plaque relative to the lumen. *Ex vivo* [PET/CT] was performed at 0, 6 and 12 weeks post-commencement of HCD using a protocol similar to that which has been for human atherosclerotic samples [1]. Briefly, the aortas were incubated with 103–127 kBq/ml [^{18}F]NaF in phosphate buffered saline (PBS) for 30 min and washed twice in PBS. The tissue was then placed in the scanner and a 30 min PET scan performed using 3-dimentional 1:5 mode. A CT scan (semi-circular full trajectory, maximum field of view, 720 projections, 50 kVp, 300 ms and 1:4 binning) was acquired for attenuation correction and quantification of macro-calcification. Scans were reconstructed using Mediso's iterative Tera-Tomo 3D reconstruction algorithm as with the *in vivo* studies.

PET data was analysed using PMOD version 3.8 (PMOD Technologies, Switzerland). For *in vivo* PET scans, micro-calcification ([^{18}F]NaF signal) was assessed in the ascending portion of the aortic arch by placing a volume of interest (VOI) around hotspots of activity. If no hotspot was present, a VOI was placed in an equivalent area of the ascending aortic arch. Background activity in the blood was assessed by placing a VOI within the left ventricle. The average [^{18}F]NaF binding at 30–60 mins (point at which equilibrium was reached) was then quantified and a tissue-to-background ratio (TBR_{mean}) was calculated. For assessment of *ex vivo* samples VOIs were placed around the arch and descending aorta before the average [^{18}F]NaF signal was quantified and normalised to radiotracer incubation dose. Macro-calcification was quantified on CT by thresholding the Hounsfield units to 200–5000, representing the range for calcified tissue and bone, and averaging the top 5 voxels. All data is presented as the mean ± standard error of the mean (SEM), with unpaired *t*-test and one-way ANOVA with post-hoc Tukey's comparison performed using Graphpad Prism v6.

https://doi.org/10.1016/j.ijcha.2020.100672

3. Results

In vivo PET/CT demonstrated that micro-calcification was present in the ascending portion of the aortic arch in all 12 week animals (Fig. 1.A). The TBR_{mean} in this portion of the aorta was twice that of the 6 week cohort (Fig. 1B). The progression of aortic micro-calcification detected by *in vivo* imaging was then validated using *ex vivo* PET/CT. $ApoE^{-/-}$ mice culled at 10–12 weeks of age prior to commencement of HCD (0 weeks) were used as a control group. Histological analysis (Masson's trichrome) on sections of the brachiocephalic branch demonstrated a continuous growth of atherosclerotic plaque over the course of 12 weeks on HCD (Fig. 1.C). *Ex vivo* [^{18}F]NaF PET/CT revealed a pattern consistent with the *in vivo* data. Micro-calcification was mainly present after 12 weeks on HCD and mostly confined to the aortic arch (Fig. 1D & E). No increase in micro-calcification was evident in the descending aorta (Fig. 1D & E). Macro-calcification was visually present on the CT scans of 3 out of the 6 animals at 12 weeks HCD and followed a similar pattern to micro-calcification (Fig. 1E & F).

4. Discussion

In this study, we have identified a preclinical model which can now be used as a non-invasive quantitative tool to investigate the development of micro-calcification in atherosclerosis. We have demonstrated that $ApoE^{-/-}$ mice fed a HCD develop micro-calcification within the aortic arch after 12 weeks which can be readily detected and quantified non-invasively using [^{18}F]NaF PET/CT. Concurrent to this study, a similar conclusion has been demonstrated by another group using *ex vivo* PET [7]. Our study is the first report which fully characterises the temporal nature of this plaque feature from onset, which is essential for development of prevention or intervention designs. This study also presents a design which facilitates longitudinal assessment of micro-calcification

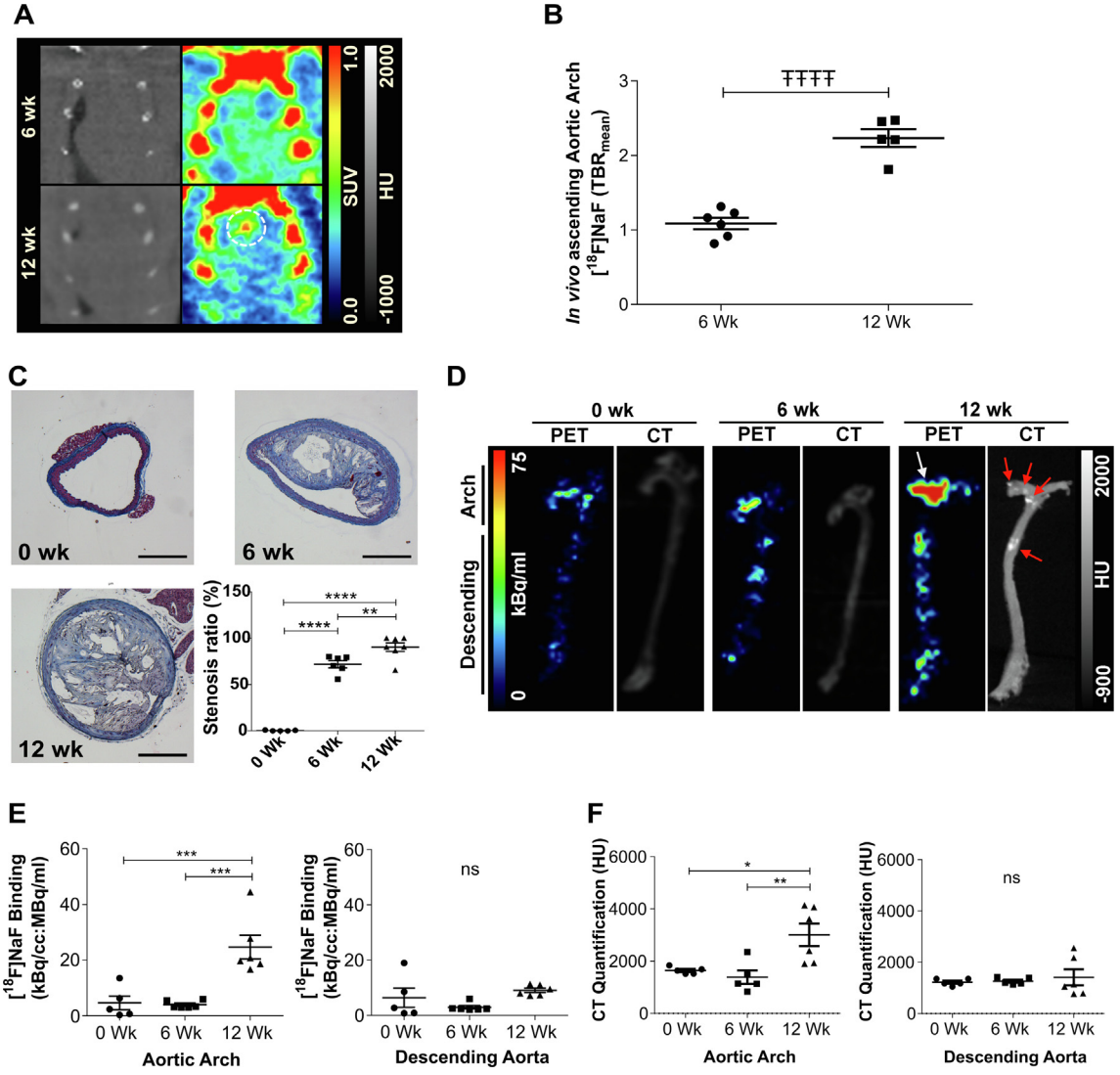

Fig. 1. Temporal characterisation of atherosclerotic micro-calcification in $ApoE^{-/-}$ HCD atherosclerosis model using [^{18}F]NaF PET/CT. (A) *In vivo* [^{18}F]NaF PET/CT of the heart and aortic arch showing micro-calcification (broken circle) in the ascending portion of the aorta within the 12 week HCD cohort. (B) Quantification of the *in vivo* PET signal within the ascending aortic arch, n = 5–6. (C) Masson's trichrome staining within the brachiocephalic trunk indicating the presence of atherosclerotic plaques from 6 weeks on HCD, progressing to a more advanced plaque by 12 weeks HCD, n = 5–6. Scale bar = 250 μm. (D) *Ex vivo* [^{18}F]NaF PET/CT showing the presence of micro-calcification (white arrow) and early macro-calcification (red arrows) mainly in the aortic arch after 12 weeks HCD. (E-F) *Ex vivo* PET and CT quantification confirmed this pattern, n = 5–6. All results are shown as the mean ± SEM, ~~TTTT~~= $p \leq 0.0001$ using an unpaired *t*-test; *=$p < 0.05$, **=$p \leq 0.01$, ***=$p \leq 0.001$ and ****= $p \leq 0.0001$ using a one-way ANOVA with post-hoc Tukey's comparison. (For interpretation of the references to colour in this figure legend, the reader is referred to the web version of this article.)

through intraperitoneal administration of [^{18}F]NaF rather than the traditional intravenous administration route for these types of radiotracers which can be challenging over multiple imaging sessions. This is in addition to a robust, non-invasive *in vivo* imaging and analysis approach which can be further validated by *ex vivo* molecular imaging. These mice also develop macro-calcified lesions as has been reported in previous studies using aged ApoE$^{-/-}$ mice [6]. With the emerging research interest in the use of anti-calcific agents preclinically [8] and clinically (ClinicalTrials.gov Identifier: NCT02132026) in the context of vascular calcification, the field lacks a characterised and validated model for assessment of novel therapies including the consequences of calcium modulation on plaque phenotype. The model presented in this study fulfils this unmet need.

The main limitation of this approach is the lack of ability to directly assess plaque rupture, as murine atherosclerotic models generally do not exhibit this feature [9]. However, this model does allow investigations into the impact of calcium modulation on plaque composition which will directly inform our translational approaches. In summary, this model can now serve as a timely and quantifiable research tool in the assessment of intraplaque micro-calcification in atherosclerosis.

5. Sources of Funding

This work is supported by Wellcome-UoE Institutional Strategic Support Fund award (ISSF2 J22738), British Heart Foundation (RG/16/10/32375 and FS/19/34/34354).

Declaration of Competing Interest

The authors report no relationships that could be construed as a conflict of interest.

References

[1] M.D. Creager, T. Hohl, J.D. Hutcheson, A.J. Moss, F. Schlotter, M.C. Blaser, M.-A. Park, L.H. Lee, S.A. Singh, C.J. Alcaide-Corral, A.A.S. Tavares, D.E. Newby, M.F. Kijewski, M. Aikawa, M. Di Carli, M.R. Dweck, E. Aikawa, Circ. Cardiovasc. Imaging 12 (2019).
[2] A. Kelly-Arnold, N. Maldonado, D. Laudier, E. Aikawa, L. Cardoso, S. Weinbaum, Proc. Natl. Acad. Sci. 110 (2013) 10741–10746.
[3] A. Irkle, A.T. Vesey, D.Y. Lewis, J.N. Skepper, J.L.E. Bird, M.R. Dweck, F.R. Joshi, F.A. Gallagher, E.A. Warburton, M.R. Bennett, K.M. Brindle, D.E. Newby, J.H. Rudd, A. P. Davenport, Nat. Commun. 6 (2015) 7495.
[4] K. Paydary, M.-E. Revheim, S. Emamzadehfard, S. Gholami, S. Pourhassan, T.J. Werner, P.F. Høilund-Carlsen, A. Alavi, Eur. Radiol. (2020).
[5] E. Aikawa, M. Nahrendorf, J.L. Figueiredo, F.K. Swirski, T. Shtatland, R.H. Kohler, F.A. Jaffer, M. Aikawa, R. Weissleder, Circulation 116 (2007) 2841–2850.
[6] J.J. Hsu, F. Fong, R. Patel, R. Qiao, K. Lo, A. Soundia, C.-C. Chang, V. Le, C.-H. Tseng, L.L. Demer, Y. Tintut, J. Nucl. Cardiol. (2020).
[7] Y. Hu, P. Hu, B. Hu, W. Chen, D. Cheng, H. Shi, Int. J. Cardiovasc. Imaging (2020).
[8] A.E. Schantl, A. Verhulst, E. Neven, G.J. Behets, P.C. D'Haese, M. Maillard, D. Mordasini, O. Phan, M. Burnier, D. Spaggiari, L.A. Decosterd, M.G. MacAskill, C.J. Alcaide-Corral, A.A.S. Tavares, D.E. Newby, V.C. Beindl, R. Maj, A. Labarre, C. Hegde, B. Castagner, M.E. Ivarsson, J.-C. Leroux, Nat. Commun. 11 (2020) 721.
[9] M. von Scheidt, Y. Zhao, Z. Kurt, C. Pan, L. Zeng, X. Yang, H. Schunkert, A.J. Lusis, Cell Metab. 25 (2017) 248–261.

Mark G. MacAskill [a,b,1]
Wendy McDougald [a,b,1]
Carlos Alcaide-Corral [a,b,1]
David E. Newby [a,1]
Adriana A.S. Tavares [a,b,1]
Patrick W.F. Hadoke [a,1]
Junxi Wu [a,c,1,*]
[a] *University/BHF Centre for Cardiovascular Science, University of Edinburgh, Edinburgh, UK*
[b] *Edinburgh Imaging, University of Edinburgh, Edinburgh, UK*
[c] *Department of Biomedical Engineering, University of Strathclyde, Glasgow, UK*
* Corresponding author.
E-mail address: junxi.wu@strath.ac.uk (J. Wu)
Received 10 August 2020
Received in revised form 20 October 2020
Accepted 28 October 2020

[1] This author takes responsibility for all aspects of the reliability and freedom from bias of the data presented and their discussed interpretation.